Title

Altered Redox Mitochondrial Biology in the Neurodegenerative Disorder Fragile X-Tremor/Ataxia Syndrome: Use of Antioxidants in Precision Medicine

Journal

Molecular Medicine, 22(1)

ISSN

1076-1551

Authors

Song, Gyu

Napoli, Eleonora

Wong, Sarah

et al.

Publication Date

2016

DOI

10.2119/molmed.2016.00122

MolecularMedicine

Altered Redox Mitochondrial Biology in the Neurodegenerative Disorder Fragile X-Tremor/Ataxia Syndrome: Use of Antioxidants in Precision Medicine

Gyu Song,[1#] Eleonora Napoli,[1#] Sarah Wong,[1] Randi Hagerman,[2,3] Siming Liu,[1] Flora Tassone,[2,4] and Cecilia Giulivi[1,2]

[1]Department of Molecular Biosciences, School of Veterinary Medicine, Davis, California, United States of America; [2]Medical Investigations of Neurodevelopmental Disorders (MIND) Institute, University of California Davis, California, United States of America; [3]Department of Pediatrics, University of California Davis Medical Center, Sacramento, California, United States of America; and [4]Department of Biochemistry and Molecular Medicine, School of Medicine, University of California, Davis, California, United States of America

A 55–200 expansion of the CGG nucleotide repeat in the 5′-UTR of the fragile X mental retardation 1 gene (*FMR1*) is the hallmark of the triplet nucleotide disease known as the "premutation" as opposed to those with >200 repeats, known as the full mutation or fragile X syndrome. Originally, premutation carriers were thought to be free of phenotypic traits; however, some are diagnosed with emotional and neurocognitive issues and, later in life, with the neurodegenerative disease fragile X-associated tremor/ataxia syndrome (FXTAS). Considering that mitochondrial dysfunction has been observed in fibroblasts and post-mortem brain samples from carriers of the premutation, we hypothesized that mitochondrial dysfunction-derived reactive oxygen species (ROS) may result in cumulative oxidative-nitrative damage. Fibroblasts from premutation carriers (n = 31, all FXTAS-free except 8), compared with age- and sex-matched controls (n = 25), showed increased mitochondrial ROS production, impaired Complex I activity, lower expression of MIA40 (rate-limiting step of the redox-regulated mitochondrial-disulfide-relay-system), increased mtDNA deletions and increased biomarkers of lipid and protein oxidative-nitrative damage. Most of the outcomes were more pronounced in FXTAS-affected individuals. Significant recovery of mitochondrial mass and/or function was obtained with superoxide or hydroxyl radicals' scavengers, a glutathione peroxidase analog, or by overexpressing MIA40. The effects of ethanol (a hydroxyl radical scavenger) were deleterious, while others (by *N*-acetyl-cysteine, quercetin and epigallocatechin-3-gallate) were outcome- and/or carrier-specific. The use of antioxidants in the context of precision medicine is discussed with the goal of improving mitochondrial function in carriers with the potential of decreasing the morbidity and/or delaying FXTAS onset.

Online address: http://www.molmed.org
doi: 10.2119/molmed.2016.00122

INTRODUCTION

A 55-200 expansion of the CGG repeat in the 5′-UTR of the fragile-X mental retardation 1 gene (*FMR1*) constitutes the genetic hallmark of premutation carriers (1). Affected subjects have increased risk of developing emotional and neurocognitive issues (2–5), primary ovarian insufficiency (6) and later in life the neurodegenerative disorder fragile X-associated tremor/ataxia syndrome (FXTAS) (1), characterized by progressive gait ataxia, intention tremor (7,8), cognitive and executive function deficits and in some cases dementia (5,9).

Unlike the full mutation alleles, which undergo repeat-mediated gene silencing (10,11), premutation alleles are active and *FMR1* mRNA levels are normal or elevated (12–14). Several mechanisms have been put forward to explain how premutation alleles might trigger neurodegeneration, including a gain-of-function (toxicity) RNA (15,16), sequestration of factors important for cell function by the "excess" of *FMR1* transcript (17,18) and translation of aberrant and toxic polyGFMR1 protein (19). While bioenergetics deficits—evidenced as mitochondrial dysfunction, abnormal mitochondrial morphology and/or dynamics—have been observed in samples from carriers

[#]*GS and EN contributed equally to this work.*
***Address correspondence to** Cecilia Giulivi, University of California, Department of Molecular Biosciences, 3009 Vet Med 3B, 1089 Veterinary Medicine Dr., Davis, CA 95616, USA. Phone: +1-530-754 8603; Fax: +1-530-754 9342; E-mail: cgiulivi@ucdavis.edu.*
Submitted May 6, 2016; Accepted for Publication June 23, 2016; Published Online (www.molmed.org) June 30, 2016.

Feinstein Institute for Medical Research
Northwell Health™

as well as in Knock-in (KI) mouse models of the premutation (20–25), our own reports have shown bioenergetic deficits accompanied by increased oxidative stress biomarkers in post-mortem brain samples (24) and fibroblasts from carriers (21,24). The mitochondrial dysfunction in fibroblasts from carriers was accompanied by lower content of Mn-superoxide dismutase (MnSOD) (24) and higher nitrative damage to the mitochondrial ATPase β-subunit (24). These mitochondrial deficits preceded the occurrence of ubiquitin-positive intranuclear inclusions (considered a hallmark of FXTAS (26)), and correlated with both CGG repeat expansion and severity of the phenotype (21,24,27).

Currently, it is not clear how mitochondrial dysfunction and/or oxidative stress might influence the onset, severity or trajectory of the clinical presentation of the premutation. However, a shift in the balance between oxidative/nitrative stress and antioxidant defenses might trigger a feed-forward cycle of more mitochondrial damage (Figure 1A), with the potential to be compounded by environmental exposures (1,28).

We hypothesized that the mitochondrial dysfunction observed in premutation carriers could result in increased oxidative/nitrative stress, opening the door for the potential use of antioxidant treatments to minimize mitochondrial damage. Direct beneficial effects would be expected, particularly to the brain, which is essentially fueled by mitochondrial ATP. To explore this hypothesis, the redox biology status in primary dermal fibroblasts from premutation carriers (Table 1) was evaluated along with the mechanisms by which its modulation via antioxidant treatments may be protective. To date, no systematic study has investigated these issues in premutation carriers, although mitochondria and antioxidant defense cross-talk likely contributes to the neuronal damage observed in other neurodegenerative/neurological diseases including Alzheimer's, Parkinson's, autism and bipolar disorders (29).

MATERIALS AND METHODS

Subjects

The study was carried out at the MIND Institute and approved by the Institutional Review Board (IRB) ethics committee at UC Davis Medical Center. Skin biopsies were obtained from 31 premutation carriers aged 8 to 67 years (mean ± SD: 41 ± 18 years) who were recruited through the Fragile X Treatment and Research Center at the MIND Institute at University of California, Davis, and who signed consent and participated in our genotype–phenotype study of families with fragile X between the years 2013 and 2015. Fibroblasts from 25 age- and sex-matched controls, aged 7 to 63 years (mean ± SD: 32 ± 17 y) were either obtained from the Coriell Institute (n = 5; Camden, NJ) or from skin biopsies obtained from volunteers recruited at the MIND Institute upon signing an informed consent (n = 20). Eight of the premutation carriers were diagnosed with FXTAS at various stages ranging from 1 to 3 (named as premutation-symptomatic or PS; Table 1). The CGG repeat number (mean ± SD: 104 ± 35 and 29 ± 5 respectively for premutation and controls) in all individuals included in this study was measured from dried blood spots using Southern Blot and polymerase chain reaction (PCR) analysis (30). The average CGG repeats of the mutant allele in heterozygous carriers (females only because *FMR1* is an X-linked gene) was 88 ± 21 (mean ± SD), significantly different from that of hemizygous carriers (males only; 117 ± 39; p = 0.009).

Cell Culture Conditions

Fibroblasts for this study were obtained from skin biopsies and cultured as previously described (21). Cell counts and viability were quantified upon addition of Trypan Blue with the use of a TC20 automated cell counter (Bio-Rad). Doubling times of, respectively, 48 ± 9 and 35 ± 7 h (p = 0.07) were recorded for controls and premutation fibroblasts. Fibroblasts from carriers did not show signs of apoptosis as judged by trypan blue staining (98 ± 2 % viability for both controls and premutation), index of loss of membrane integrity. Cell morphology did not show any obvious difference in term of shrinkage (hallmark of apoptosis) in fibroblasts from carriers compared with controls (not shown). For outcomes evaluation, cells (1×10^6) were centrifuged at 200 g for 5 min and cell pellet homogenized and resuspended in 20 mmol/L HEPES, pH 7.4 for enzymatic activities, or RIPA (50 mmol/L Tris-HCl, 150 mmol/L NaCl, 2 mmol/L EDTA, 0.5% CA-630 octylphenoxypolyethoxyethanol, 0.1% sodium dodecyl sulfate (SDS), 0.012% deoxycholate, 0.5% Triton X-100, pH 7.4) for Western blotting. Both solutions were supplemented with protease and phosphatase inhibitors. Protein concentration was determined with a Pierce BCA protein assay kit (Life Technologies) according to the manufacturer's instructions. Measurements were performed on a Tecan Infinite M200 microplate reader equipped with the Magellan data analysis software (Tecan).

Antioxidants Treatment

Cells (1×10^6) were grown at 37°C in 5% CO_2 for 24 h. After 48 h fresh media were added to the cells with the following antioxidants: Trolox (a water-soluble vitamin E analog, 1 mmol/L), quercetin (10 μmol/L), epigallocatechin gallate (EGCG, 10 μmol/L), ethanol (31–37); 0.1%) and dimethyl sulfoxide (DMSO, 0. 1%), as hydroxyl radical quenchers; the cell-permeable superoxide dismutase (SOD) mimetic Mn^{3+}tetrakis (4-benzoic acid) porphyrin (MnTBAP, 50 μmol/L), to quench superoxide anion and prevent the formation of the highly reactive peroxynitrite (product of superoxide anion and nitric oxide); L-ascorbic acid (1 mmol/L), to increase the reducing capacity of the cells to counteract oxidative conditions and reduce sulfenic acid in Cys-containing proteins; the cell permeable glutathione precursor *N*-acetyl-L-cysteine (NAC) (1 mmol/L) to increase the synthesis of glutathione

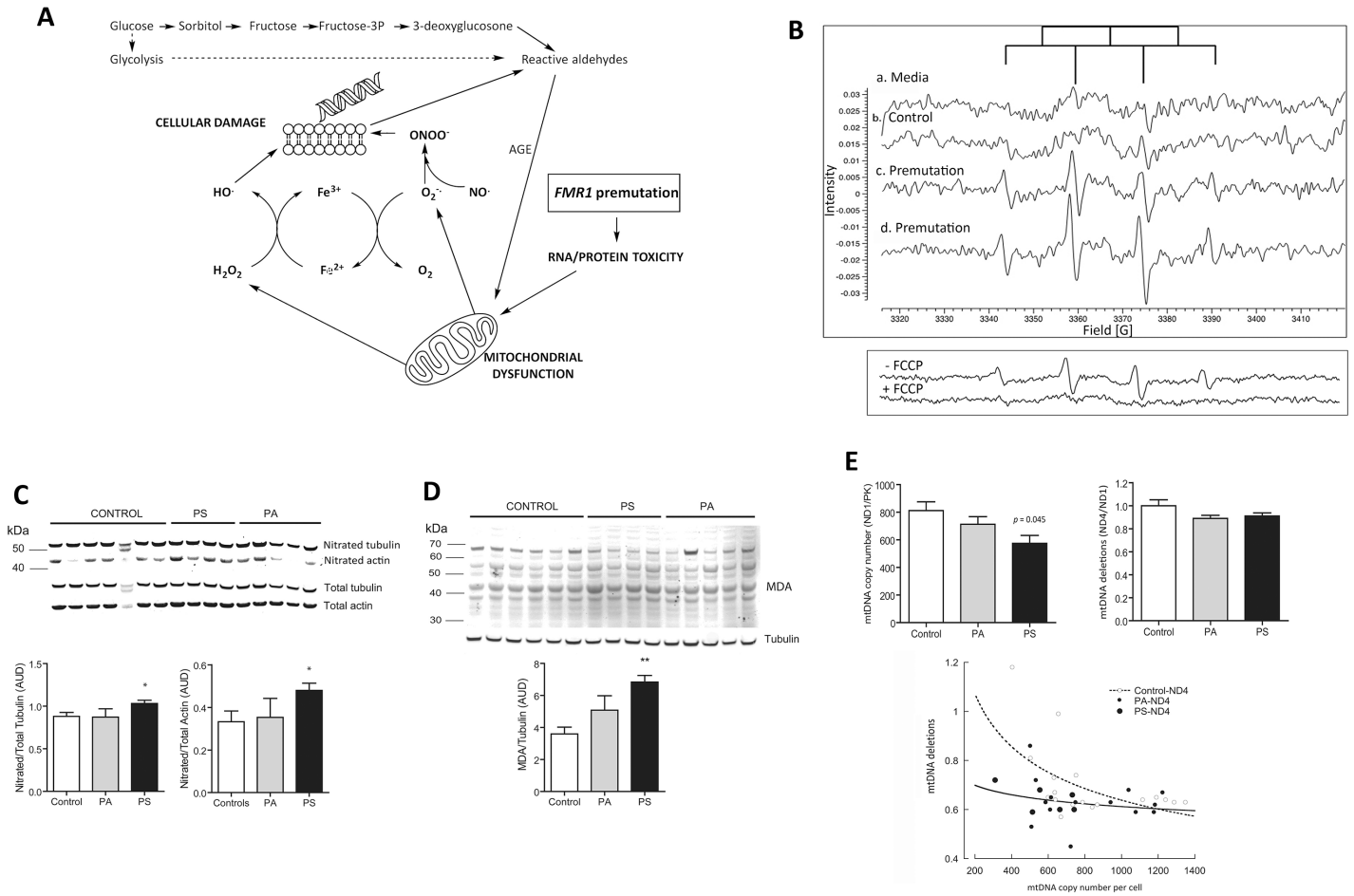

Figure 1. Redox biology pathways in premutation carriers. (A) Increases in mitochondria-derived superoxide anion production can lead to the formation of the highly reactive species resulting in biomolecule damage. In parallel, hyperactivation of the polyol pathway—usually associated with mitochondrial dysfunction—leads to excessive accumulation of sorbitol and fructose contributing to increases in cytosolic (NADH)/(NAD^+) ratios reducing the glucose flux via glycolysis and pentose phosphate pathway. This scenario impacts the mitochondrial (NADH)/(NAD^+) leading to the generation of "reactive aldehydes" and oxidatively modified proteins or advanced glycation end-products. (B) Electron paramagnetic detection of free radicals in fibroblasts. Aliquots of cells from control and two premutation donors supplemented with deferoxamine, DMSO and DMPO were taken within 10–15 min after the addition of the spin trap. A weak EPR background signal was detected with cell culture media alone (a), which was higher upon addition of control cells (b). This latter signal was constituted by a quartet with an intensity ratio of 1:2:2:1 and hyperfine splitting constants $a^N = a^{H\beta} = 14.9$ G for N and H^β consistent with the detection of DMPO-hydroxyl radical adduct, further confirmed by spectra simulation. Cells from two premutation carriers exhibited EPR spectra similar to that of controls constituted solely by hydroxyl radical (c) or by a combination of hydroxyl and a second adduct at a ratio of 19 to 1 (d). This secondary adduct ($a^N = 16.4$ G and $a^{H\beta} = 23.3$ G) indicated the presence of DMPO-methyl adduct which resulted from the quenching of methyl radical (formed from the reaction between hydroxyl radical and DMSO) by DMPO. Lower panel: Representative EPR spectra of a cell line from a carrier with and without the addition of FCCP. (C) Representative Western blot image of 3-nitrotyrosine content in tubulin and actin of fibroblasts from controls, asymptomatic (PA) and FXTAS-affected or symptomatic (PS) premutation carriers. Intensity of nitrated actin and tubulin (expressed as arbitrary units of densitometry, AUD) were normalized by their respective total protein. ANOVA followed by Bonferroni was performed when comparing controls, PA and PS. $^*p < 0.05$ versus controls. (D) Representative Western blot image and correspondent densitometry of MDA-protein adducts from controls and FXTAS-affected (PS) and unaffected (PA) carriers. ANOVA followed by Bonferroni's *post hoc* test was used for the statistical analysis. $^*p < 0.005$ versus controls. (E) Mitochondrial DNA copy number and deletions in control and premutation fibroblasts and correlations between these outcomes. *P* values were obtained with ANOVA followed by Bonferroni's *post hoc* test. For correlations: Pearson's *r* value = –0.500 and –0.244 ($p = 0.034$ and 0.230) for controls and premutation respectively.

and improve the activity of the glutathione peroxidase-reductase system; and the glutathione peroxidase analog Ebselen (1 μmol/L) to improve the capacity to catabolize organic hydroperoxides. DMSO, ethanol, ascorbic acid and NAC were dissolved in cell culture media, all other chemicals were dissolved in DMSO (final concentration in media = 0.1% V/V). For these experiments and cell density, the concentration of DMSO was equivalent to 0.2 nmol × $(cell)^{-1}$.

Complex I, Complex IV and Citrate Synthase Activities

Measurements of specific activities were carried out spectrophotometrically in a Tecan Infinite M200 microplate reader equipped with the Magellan software as previously described. (24,38). Details on the evaluation of Complex I, Complex IV and citrate synthase activities are included in the Supplementary Methods.

Western Blotting

Cells were lysed in RIPA buffer and proteins were denatured in NuPAGE sample buffer (Life Technologies) plus 50 mmol/L dithiothreitol at 70°C for 10 min as described (38). Primary antibodies were: anti-COXIV (MitoSciences, Eugene, OR; 1:1,000 dilution), anti-COX17, anti-cytochrome *c*, anti-GFER, anti-MIA40, anti-NDUFB7, anti-VDAC (all from Proteintech; 1:1,000 dilution), anti-nitrotyrosine (Abcam; 1:500 dilution) and anti-malondialdehyde (Alpha Diagnostic Inc.; 1:500 dilution). To confirm specificity of the nitration staining, membranes were stripped with the New Blot IR stripping buffer (LI-COR) for 30 min at 30°C, washed three times in distilled water and treated with 100 mmol/L dithionite in 50 mmol/L sodium borate buffer (pH 9) for 2 h at room temperature to reduce the nitro group into an amino group, preventing the antibody from binding with the nitrated moiety. Anti-β-actin (Sigma-Aldrich; 1:30,000 dilution) and anti-α-tubulin (Cell Signaling Technologies; 1:1,500 dilution) antibodies were used as loading controls. Secondary

Table 1. Characteristics of the donors of fibroblasts utilized in this study.

ID	Age (y)	CGG	Sex	Outcome
		CONTROLS		
C1	7	26	M	mtDNA
C2	8	30	M	CS, EPR, Metabol, mtDNA
C3	10	30	M	CS, Metabol, mtDNA, VDAC
C4	12	34	M	ACT, MDRS, OE, Metabol, mtDNA
C5	16	21	M	NT, MDA, mtDNA
C6	18	23	M	ACT, MDRS, Metabol, mtDNA
C7	20	29	M	ACT, mtDNA
C8	23	29, 30	F	NT, MDA, mtDNA
C9	24	30	M	NT, MDA, mtDNA
C10	25	29	M	NT, MDA, mtDNA
C11	26.3	30, 37	F	mtDNA
C12	29	30	M	NT, MDA, mtDNA
C13	29.1	29	M	ACT, MDRS, mtDNA
C14	33.7	23, 30	F	mtDNA
C15	34	N/A	M	mtDNA
C16	34	29	F	CS, mtDNA, VDAC
C17	36	30	M	ACT, MDRS, mtDNA, VDAC
C18	39	N/A	F	CS, Metabol
C19	40	N/A	F	CS, Metabol, mtDNA
C20	41.2	43	M	ACT, mtDNA
C21	46	N/A	F	ACT, Metabol
C22	59	21	M	mtDNA
C23	61	30	M	NT, MDA, mtDNA
C24	62	30	M	NT, MDA, mtDNA
C25	63	22	M	mtDNA
		ASYMPTOMATIC PREMUTATION		
PA1	8.4	150, 180	M	ACT, CS, EPR, Metabol, mtDNA, VDAC
PA2	8.4	157, 180	M	ACT, CS, EPR, Metabol, mtDNA, VDAC
PA3	9.7	31, 63	F	mtDNA
PA4	17.1	170	M	ACT, MDRS
PA5	17.3	16, 67	F	mtDNA
PA6	23.4	77	M	ACT, MDRS, OE
PA7	24	31, 93	F	mtDNA
PA8	24	30, 79	F	mtDNA
PA9	25	72	M	ACT, NT, MDA, mtDNA
PA10	33.1	30, 137	F	NT, MDA, mtDNA
PA11	33.5	133	M	VDAC
PA12	37	43, 78	F	CS, VDAC, Metabol, mtDNA
PA13	38.4	33, 60	F	NT, MDA, mtDNA
PA14	40.8	127	M	MDRS, mtDNA
PA15	40.8	150	M	NT, MDA
PA16	43	106	F	mtDNA
PA17	49.3	31, 86	F	NT, MDA, mtDNA
PA18	49.9	20, 98	F	VDAC, mtDNA
PA19	52	29, 81	F	mtDNA
PA20	54	133	M	ACT, MDRS, mtDNA, VDAC
PA21	55.4	30, 69	F	mtDNA
PA22	55.6	104	M	mtDNA
PA23	56	81	M	ACT, MDRS, mtDNA
		SYMPTOMATIC PREMUTATION		
PS1 (Stage N/A)	54	133	M	MDRS
PS2 (Stage N/A)	56	81	M	MDRS

Continued on the next page

Table 1. ***Continued.***

PS3 (Stage 3)	59.1	33,107	F	ACT, NT, MDA, mtDNA
PS4 (Stage 1)	61.8	110,130	M	ACT, NT, MDA, mtDNA
PS5 (Stage 4)	62.5	105	M	VDAC, NT, MDA, mtDNA
PS6 (Stage 3)	63.0	102	F	mtDNA
PS7 (Stage 1)	63.1	60	M	ACT, VDAC, NT, MDA, mtDNA
PS8 (Stage N/A)	67	79	M	MDRS

All samples were tested for polarography and citrate synthase activities. Other outcomes evaluated in each of the samples are indicated in the last column, for not all samples were available on a timely manner or their yield was limiting for some of the analyses. Western blots for voltage-dependent anion channel (VDAC), malondialdehyde crosslinked to Lys-containing proteins (MDA); nitrotyrosine (NT); citrate synthase activity before and after antioxidants treatment (CS); MDRS indicates the Western blots performed for selected proteins (namely, COX17, NDUFB7, MIA40, GFER and cytochrome *c*); overexpression of MIA40 (OE); identification and detection of oxygen-centered free radicals performed by electron paramagnetic resonance with the addition of spin tra*p* (EPR); metabolomics studies (Metabol); mtDNA indicates evaluation of mtDNA copy number and deletions; Complex I, IV and citrate synthase activities (ACT). Abbreviations: N/A = not available.

antibodies were IRDye 800CW goat anti-rabbit antibody (LI-COR; 1:10,000 dilution) or 680 goat anti-mouse antibody (LI-COR; 1:10,000 dilution). Proteins were visualized by Odyssey infrared imaging system (LI-COR) scanning at 700 and 800 nm. Quantification of the net intensities for all bands was carried out with the use of the Carestream software (Carestream).

Electron Paramagnetic Resonance (EPR) Conditions

Primary fibroblasts (5×10^5 cells) from two controls and three premutation carriers were plated in a T75 flask and grown overnight as stated above. The next day, cells were washed with PBS and 3 mL of RPMI 1640 medium (without phenol red) supplemented with 15% FBS, 2 mmol/L glutamine, 1 mmol/L sodium pyruvate, 0.1% DMSO, 5 μmol/L deferoxamine mesylate and 90 mmol/L DMPO (Dojindo Molecular Technologies). Cells were incubated at 37°C in a 5% CO_2 atmosphere. After 5–15 min, a 150-μL aliquot of the supernatant was transferred to a sealed bottom glass Pasteur pipette and placed into the cavity of an Elexsys 3500 EPR spectrometer (Bruker). The scans were taken at room temperature. After the first aliquot, all others were taken every hour up to 2 h. The spectra were obtained with a single scan using the following instrument parameters: receiver gain = 70 db; modulation amplitude = 0.5 G; modulation frequency = 100 kHz; resolution = 1,024 points; center field = 3,368 G; sweep width = 100 G; time constant = 1,310.72 ms; sweep time = 335.54 s; and microwave pow*e*r = 20 mW. Analyses of radical products were done using the Bruker Xepr software to determine area and peak height of signals and the identification of adducts was performed with the simulation software Xepr (version 2.6b87, Bruker).

Mitochondrial DNA Copy Number and Deletions

The mtDNA copy number estimated by evaluating the mtDNA/nDNA gene ratio was determined using qPCR as described (39). The mtDNA copy number in each cell was expressed as the ratio between a mitochondrial gene (*ND1*) and the single-copy nuclear *PK* whereas deletions were calculated as the gene ratios of *ND4* over *ND1*. Other experimental details were given in the Supplementary Methods.

Metabolomics of Cultured Fibroblasts

Metabolomics analysis was carried out as described in detail previously (40). Metabolites were identified by matching the ion chromatographic retention index, accurate mass and mass spectral fragmentation signatures with reference library entries created from authentic standard metabolites under the identical analytical procedure as the experimental samples. Details on data acquisition chromatographic parameters, data processing and statistical analysis are reported in the Supplementary Methods.

Overexpression of MIA40

Plasmids pCMV6-hMIA40 (Human *MIA40* expressing vector, OE) and pCMV6-EV (empty or noncoding vector control, EV) were purchased from Origene (Rockville). Fibroblasts from a control and a carrier were cultured in regular medium. On d 1, 4×10^6 cells were seeded into each of two 6-cm dishes (one EV and one OE). On d 2, cells at 90% confluency were ready for transfection. For the transfection, 8 μg of plasmid DNA (EV or OE) in 250 μL Opti-MEM (Reduced Serum Medium, Life Technologies) was mixed with 12 μL of Lipofectamine 2000 (Life Technologies) in 250 μL of Opti-MEM. Medium was removed from the cells and replaced with the DNA-Lipofectamine mixture-supplemented medium and incubated at 37°C. After 14 h of incubation, the transfection medium was replaced by regular medium. After 48 h, cell viability was assessed and cell homogenates prepared to test for MIA40 expression levels and Complex I and citrate synthase activities. Transfection experiments were run four different times and in biological duplicates.

Confocal Microscopy

Cells (1×10^5) were seeded on sterile coverslips and stained with 0.5 μmol/L MitoTracker Red CMXRos (Molecular Probes Inc.) as previously described (41). Images of fixed cells were obtained with an Olympus FV1000 laser scanning confocal microscope (excitation and emission wavelengths 594 and 660 nm, respectively) at 60 × magnification.

Statistical Analysis

Experiments were run in triplicates for each cell line (unless otherwise indicated). Data were expressed as mean ± SEM and statistical analysis was performed with Student *t* test when comparing two groups and ANOVA followed by Bonferroni's *post hoc* test when comparing 3 or more groups. For proportions, the chi-square test was used without the Yates correction. For metabolomics, metabolite identification was performed as described in the Supplementary Methods.

All supplementary materials are available online at www.molmed.org.

RESULTS

Increased Mitochondrial ROS Production in *FMR1* Premutation

Primary dermal fibroblasts from premutation carriers were analyzed for reactive oxygen species production by using electron paramagnetic spectroscopy (EPR). Direct detection of some free radicals (for example, superoxide anion and hydroxyl radical) is very difficult due to their relatively low concentrations (<nmol/L), high reactivity and short half-life. To evaluate and identify oxygen-centered free radicals in these cells, we utilize the spin trapping technique. With this approach, the target free radical reacts with a spin trap (in our case 5,5′-dimethyl-1-pyrroline-*N*-oxide or DMPO) forming a stable, distinguishable free radical adduct whose spectrum then can be detected by EPR. Identification of radicals is performed by calculating hyperfine-splitting constants as well as by determining the peak numbers and intensity ratios, whereas amount of radicals is estimated by the double integration of the spectrum.

Cells from premutation carriers exhibited EPR spectra similar to that of controls (Figure 1B, a, b), but with a significantly higher intensity, constituted by one (DMPO-hydroxyl; Figure 1B, *c*) or two (DMPO-hydroxyl and DMPO-methyl at a 19:1; Figure 1B, d) signals. It is likely that the DMPO-hydroxyl signal recorded in <15 min reflected either the decay of the DMPO-superoxide ($t_{0.5}$ < 1 min) to the DMPO-hydroxyl adduct or direct trapping of hydroxyl radical by DMPO. In contrast, the DMPO-methyl adduct originates from the trapping of hydroxyl radical (produced by the metal-catalyzed H_2O_2 cleavage and subsequent trapping by DMSO) by DMPO (Supplementary Figure 1). Double integrals to estimate the total area of the signal—which is proportional to the free radicals' concentration—indicated that premutation cells exhibited a 2.4- and four-fold higher area than controls (Figures 1B, c and 1B, d). About 70% of these signals were sensitive to the mitochondrial uncoupler carbonilcyanide *p*-triflouromethoxyphenylhydrazone (Figure 1B, lower panel), which decreases both membrane potential and ROS production by mitochondria (42) suggesting a major mitochondrial contribution to the total cellular free radical pool.

Increased Biomarkers of Cellular Oxidative Stress-Mediated Damage in Premutation with Cytoskeletal Protein Nitration in FXTAS-Affected Carriers Only

By using a metabolomics approach, a total of 143 metabolites were identified in fibroblasts from carriers of the premutation and matched controls. From these, 44 metabolites were identified by the fold change analysis (See Materials and Methods and Supplementary Methods). A subset of metabolites (n = 6; 13.6% of the total number of metabolites with different abundance) was identified as being markers of oxidative stress-mediated damage to both carbohydrates and proteins (Table 2). Among them, increased levels of metabolites derived from oxidation of carbohydrates (hexuronic acid from glucose) and proteins (aminomalonate) were detected by untargeted metabolomics in cells from premutation versus controls (Table 2). Interestingly, a hyperactivation of the polyol pathway was inferred by the increased levels of sorbitol (Table 2 and Figure 1A) as well as by products of glycated proteins (threonic and isothreonic acids). A decrease in the pentose phosphate shunt was supported by increased threitol levels as it is observed in individuals with ribose-5-phosphate isomerase deficiency (OMIM: 608611).

Table 2. Metabolites related to increased oxidative stress in fibroblasts from premutation carriers.

Compound	Fold change	*p* value
Hexuronic acid	1.4	0.020
Threitol	1.3	0.016
Sorbitol	1.2	0.042
Threonic acid	1.2	0.060
Aminomalonate	1.1	0.078
Isothreonic acid	1.1	0.021

A total of 143 metabolites detected by metabolomics were identified in samples from carriers of the premutation and matched controls. By using univariate analysis, 44 metabolites were identified by fold change analysis (See Materials and Methods). From these, the 6 metabolites identified as markers of oxidative stress-mediated damage to carbohydrates and proteins and relevant for this study are shown. Fold changes were expressed as LOG2 of the ratio of average values of premutation over controls. The *p* values were obtained through the Student *t* test (if the metabolites followed a normal distribution) or Kruskall-Wallis (if the metabolites followed a distribution other than normal).

Following the worsening of clinical symptoms, only cells from FXTAS-affected carriers showed significantly higher Tyr nitration (nitrotyrosine or NT) of the cytoskeleton proteins tubulin and β-actin (Figure 1C) and increased malondialdehyde (MDA) crosslinked to Lys-containing proteins (Figure 1D). Taken together, these results are consistent with higher oxidative-nitrative damage in FXTAS-affected carriers compared with controls and unaffected carriers.

Increased Mitochondrial Damage in FXTAS-Affected Carriers

To assess mitochondria-specific oxidative damage, the mitochondrial DNA copy number (mtDNA CN) and

deletions were evaluated in cells from premutation carriers. Decreased mtDNA copy number and increased deletions were observed in fibroblasts from carriers (regardless of FXTAS) versus controls (Figure 1E; control versus average of all premutation carriers with and without FXTAS; $p = 0.038$ for copy number and $p = 0.022$ for deletions). The mtDNA copy number was decreased by 25% in cells from FXTAS-affected carriers compared with controls ($p = 0.045$; Figure 1E).

Consistent with the asymmetric mtDNA replication process, in which major arc segments are not protected by the complementary strand becoming more prone to ROS-mediated damage (40), the mtDNA CN correlated with deletions in control cells (Figure 1E). However, no correlation was observed for premutation fibroblasts suggesting that accumulation of deletions in the mtDNA of carriers is not necessarily linked to the replication process, but rather acquired continuously and/or not repaired accordingly.

Impaired Redox-Regulated Mitochondrial Disulfide Relay System (MDRS) Affects Complex I Activity in Premutation Fibroblasts

The redox-sensitive MDRS participates in the import of nuclearly encoded mitochondrial proteins (Figure 2A), including some subunits of Complexes I and IV (21). Significant decreases in protein expression were observed for the MDRS members MIA40, cytochrome *c* and NDUFB7 in fibroblasts from carriers, which were magnified in FXTAS-affected individuals (Figure 2B). Complex I and IV activities (normalized by the matrix biomarker citrate synthase) in premutation fibroblasts were, respectively, 50% ($p = 0.03$; Figure 2C) and 64% ($p = 0.123$) of controls. These results are consistent with findings showing that altered ratios of MDRS components lead to deficiencies in several Complexes including I and IV (OMIM 613076) (38). To explore whether the above deficits were ascribed to increases in mitochondrial mass, intrinsic lower Complex activities or both, citrate synthase activity was evaluated (Figure 2C). While no differences were obtained in these outcomes between diagnostic groups' means, the incidence of activities < 95%CI was 57% and 75% for asymptomatic and FXTAS-affected carriers, respectively (χ^2 test $p = 0.007$).

In an attempt to rescue mitochondrial function, the redox-sensitive import receptor MIA40 was overexpressed in fibroblasts from controls and premutation individuals (Figure 2D). Confocal microscopy analysis of control fibroblasts confirmed increases in mitochondrial MIA40 expression (1.7- to 1.9-fold in coding vector versus empty vector; Figure 2E). Overexpression of MIA40 resulted in significant increases in cell viability (premutation only; Figure 2F) and Complex I activity (control and premutation) but with a 2.5-fold higher effect in premutation than controls (Figure 2F).

Specific Antioxidant Treatments Increase Mitochondrial Biomarkers of Mass and Function

The potential efficacy of several antioxidants at recovering mitochondrial mass and/or function was tested in a selected subset of fibroblasts from asymptomatic carriers (Figure 3). This set had the lowest citrate synthase activities (70.2% of controls, $p = 0.045$) and the recovery readouts were either citrate synthase activity or the expression of biomarkers of outer and inner mitochondrial membranes (voltage-dependent anion channel or VDAC and cytochrome *c* oxidase subunit IV or COXIV, respectively). Treatment of premutation fibroblasts with antioxidants quenching either superoxide anion (MnTBAP) or hydroxyl radical (dimethylsulfoxide, DMSO and Trolox), ascorbic acid (to improve reducing conditions in polar phases) and the glutathione peroxidase mimetic Ebselen restored citrate synthase activity to or above control values (Figure 3A).

Recovery of citrate synthase activity up to control values was obtained with *N*-acetyl-L-cysteine (NAC) with two of the cells from carriers, whereas one of them showed a detrimental effect (PA12). A consistent damaging effect of ethanol (tested as a putative hydroxyl radical scavenger (31–37)) on citrate synthase activity was observed for all cells from carriers (Figure 3).

Treatments with DMSO, Ebselen, Trolox, quercetin and epigallocatechin gallate (EGCG) did not improve the recovery of VDAC and COXIV relative to untreated cells (Figure 3B). The only cell line (PA12, Figure 3B, C) that showed improvements with all treatments for VDAC only was the same one that responded negatively with NAC suggesting that these treatments are both carrier- and outcome-specifics. These cells were from a FXTAS-free female carrier (PA12; Table 1) whereas those unresponsive to the treatments were from carriers either affected with FXTAS (PS5 and PS7) or older and FXTAS free but with relatively longer CGGs (PA20 and PA18; Table 1). Considering that *FMR1* is an X-linked gene, we cannot exclude that the X-chromosome activation ratio might have played a role at improving the mitochondrial outcomes in this female donor over that of others tested in which all were males except PA18.

DISCUSSION

The molecular consequence of the premutation is usually an increase in *FMR1* mRNA levels with "toxic" long repeat tracks (13) and a reduction in FMRP levels that are a function of increasing CGG repeats. Several reports favor a pathogenic mechanism that involves the effects of the premutation mRNA. These mRNA repeat tracks may lead to sequestration of proteins that bind to the repeat, thus losing their potential to function properly (reviewed in (19)). Also, these long repeat tracks may cause repeat associated non-AUG (RAN) translation, leading to a toxic polygutamine or polyalanine products (43). Although we are not aware of any study on the influence of AGG interruptions on mitochondrial dysfunction, it is known that AGG interruptions change the secondary structure of premutation mRNA transcripts (44,45)

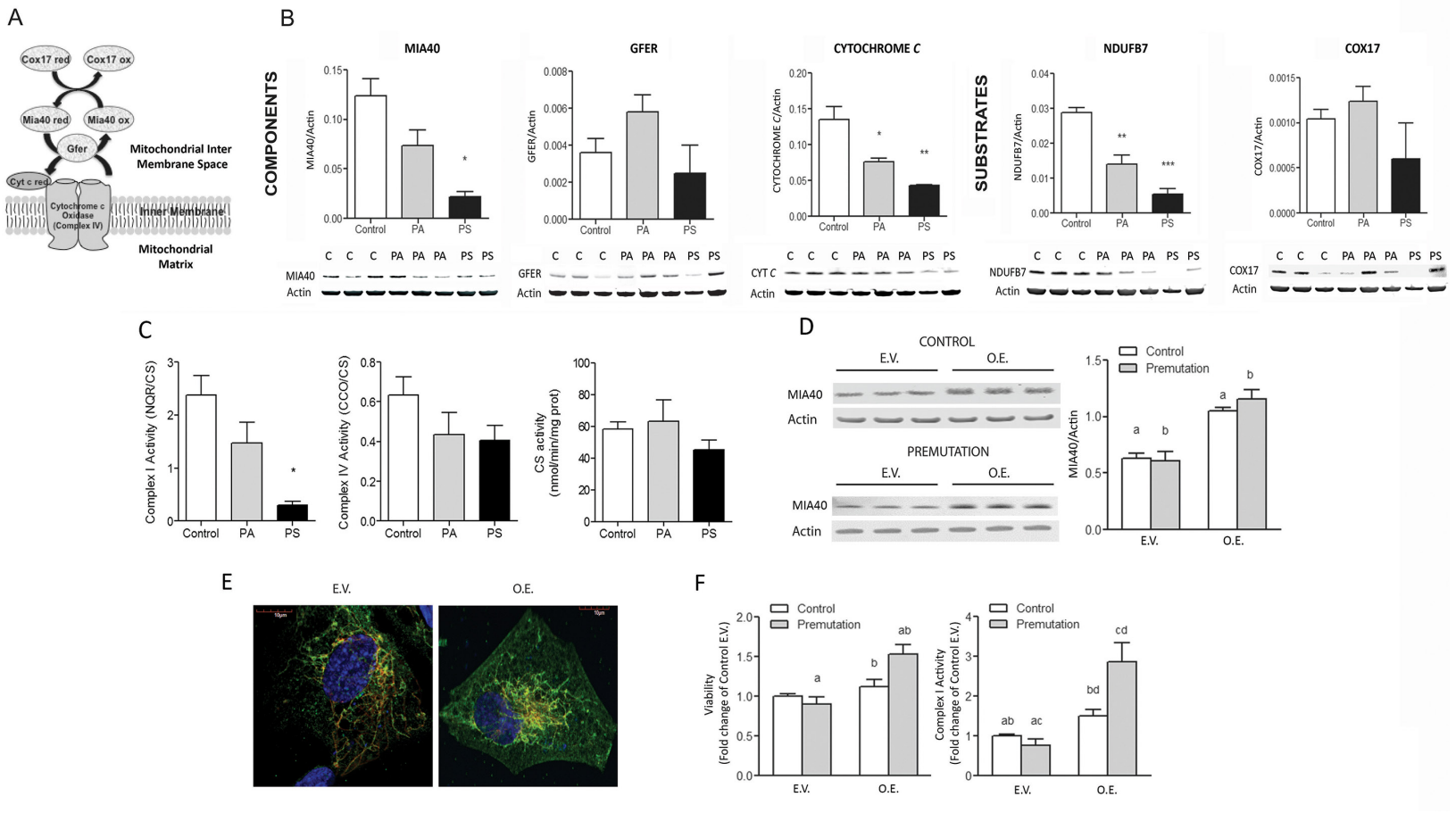

Figure 2. Mitochondrial disulfide relay system dysfunction and effect of MIA40 overexpression in fibroblasts from premutation carriers. (A) Nuclearly encoded proteins are imported into the inner membrane space and translocated in their reduced form into mitochondria. The oxidized form of MIA40 gives rise to a transient intermolecular disulfide bridge with the reduced precursor protein, resulting in oxidation of the precursor protein that now contains an intramolecular disulfide bond and is able to undergo folding in the IMS. Reduced MIA40 is then reoxidized by GFER via a disulfide relay system. Reduced GFER is reoxidized, transferring its electrons to O_2 via cytochrome *c* and cytochrome *c* oxidase, linking MDRS to respiratory chain activity (38). (B) Representative Western blot images and densitometry of the protein levels of substrates (COX17 and NDUFB7) and elements of the MDRS system (MIA40, GFER, cytochrome *c*) in cell extracts from controls, PA and PS carriers. Band intensity of the proteins of interest was normalized to actin and data are shown as mean ± SEM ($n = 4$ for control, $n = 5$ for PA, $n = 3$ for PS). Data were analyzed by ANOVA followed by Bonferroni's post-hoc test. $^{*}p < 0.05$; $^{**}p < 0.005$; $^{***}p < 0.001$ versus controls. (C) Activities of Complex I, IV and citrate synthase were evaluated in control, PA and PS. Complex I and IV activities were normalized to citrate synthase. The 95% CI for citrate synthase activity was 48-68 nmol × (min × mg protein)$^{-1}$. Statistical analysis was performed with the Student *t* test between PS and control. $^{*}p < 0.05$. (D) Two cell lines (one control and one premutation) were chosen to over-express MIA40. Cells were cultured in regular media and transfected at 90% confluency with either empty vector (E.V.) or MIA40 coding or overexpression vector (O.E.). At 48 h, MIA40 protein expression was evaluated by immunoblots in E.V. or O.E. using β-actin as the loading control. Average of 4 independent experiments. (E) Confocal images of control fibroblasts transfected with either E.V. or *MIA40* O.E. vector showing mitochondria staining and MIA40 subcellular distribution. Red = mitochondria; Green = MIA40; Yellow = overlap. (F) Cell viability (evaluated by Trypan blue exclusion) and Complex I activity (NADH-quinone reductase normalized to citrate synthase) were assessed in E.V. and O.V. Values represent the average of 4 independent experiments normalized to control values. $^{*}p < 0.05$.

A

Treatment	Citrate synthase activity [nmol x (min x mg prot)$^{-1}$]			
	PA1	PA2	PA12	95%CI; n = 5
None	59.5	53.8	34.8	54.4-73.3
Ascorbic acid	90.9	84.0	76.4	67.7-75.3
Trolox	86.9	63.4	78.3	45.7-60.8
Ebselen	75.9	73.7	71.4	41.5-72.8
DMSO	72.4	85.8	73.3	64.3-73.3
MnTBAP	81.9	87.8	64.1	57.4-86.0
NAC	45.1	46.0	28.3	41.1-53.1
Ethanol	123.4	150.0	134.7	152.4-196.1

B

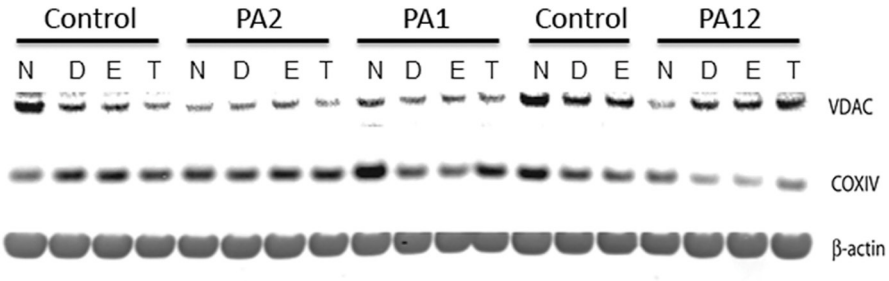

C

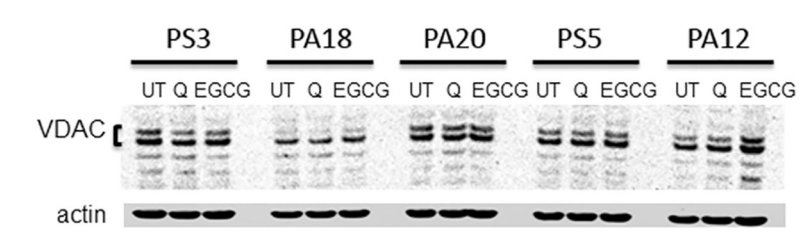

Figure 3. Effect of antioxidant treatment on the recovery of mitochondrial biomarkers. (A) Citrate synthase activity (expressed as nmol × (min × mg protein)$^{-1}$) was evaluated in untreated (media only), vehicle-treated (DMSO), and antioxidant-treated cells (n = 5 and n = 3, for controls and premutation, respectively; see Table 1) after 48 h. The 95% CIs for each treatment were performed with control values (C2–C3, C16, C18–C19). Values in red indicate below the 95% CI; in green above, and not colored within the limits of the 95% CI. (B) Representative image of a Western blot run with cells (two controls and three premutation) treated with media (none or N), DMSO (D), Ebselen (E, in DMSO) and Trolox (T, in DMSO) for 48 h and evaluated for VDAC, COXIV and β-actin (loading control) protein expression. (C) Cells from premutation donors were treated for 48 h with quercetin, EGCG or vehicle DMSO and Western blots evaluated VDAC protein expression (the doublet could be attributed to alternative spliced products).

and that these secondary structures are part of the mechanisms hypothesized to explain premutation-associated disorders (for review, see (46)). Adding to these mechanisms, bioenergetic deficits (and in some cases also with increased oxidative stress biomarkers) have been observed in post-mortem human brain samples (24) and fibroblasts from adult premutation carriers (20,21,24) as well as in isolated neurons, brain regions and granulosa cell and oocyte from a KI mouse model (25,47). Altered mitochondrial network and dynamics have been noted in fibroblasts from carriers (20) and neurons from a knock-in (KI) mouse model of *FMR1* premutation (23). These deficits precede the occurrence of ubiquitin-positive intranuclear inclusions, considered a hallmark of FXTAS (26), and correlate with both CGG repeat expansion and severity of the phenotype (21,24).

In this study, we hypothesized that mitochondrial dysfunction, and the ensuing higher ROS production, may result in cumulative oxidative-nitrative damage and that the treatment with antioxidants have the potential to recover some of the mitochondrial damage/function. In the context of the premutation, redox active metals could be sequestered in brain nuclear inclusions, aggregates of CGG repeat-associated non-AUG-initiated translation products or excess mRNA/RNA molecules (1). In this regard, altered zinc (21,27) and iron (21,22) homeostasis have been reported in premutation individuals, and the superoxide anion-mediated reduction of such redox active metals may act as catalytic centers for hydroxyl radical generation (Figure 1A). In support of this concept, addition of the iron chelator deferoxamine mesylate to fibroblasts from older (>60-year-old), FXTAS-affected carriers showed a significant improvement of Complex IV activity (1.26-fold of vehicle treated (21)).

In this study, we utilized primary fibroblasts from premutation carriers compared with age- and sex-matched controls. Although it could be argued that the use of primary dermal fibroblasts taken at a single time point may not adequately represent the individual's overall oxidative/inflammatory status or its progression over time, fibroblasts in culture allow attesting whether the observed deficits are due to the genetic defect *per se* removed from secondary to other pharmacological or pathological processes occurring in the whole organism. Furthermore, defects in mitochondrial outcomes evaluated in fibroblasts seem to mirror the ones in brain, a more relevant organ for this disorder (20–25).

Our findings point to increases in mitochondrial oxidative stress compounded by lower antioxidant defenses (lower supply of NADPH from pentose phosphate shunt), which result in further damage to mitochondria. This is supported by increases in cellular and mitochondrial oxidative stress as judged by: (i) an increased mitochondrial ROS production (two- to four-fold higher than controls) evaluated by EPR with spin trapping technique; (ii) increases in markers of oxidation of carbohydrates (hexuronic acid from glucose) and proteins (aminomalonate) with a hyperactivation of the polyol pathway and (iii) a decrease in the pentose phosphate shunt; (iv) increases in mtDNA deletions; (v) decreases in MDRS components (MIA40, cytochrome *c* and NDUFB7) accompanied by lower Complex I and IV activities.

Following the presence of FXTAS, fibroblasts from carriers of the premutation showed marked deficits in MDRS components and activities of Complexes I and IV, and more significant protein damage as evidenced by both Tyr nitration of the cytoskeleton proteins tubulin and β-actin and MDA crosslinkings. It is tempting to propose that altered cytoskeletal organization—as a result of nitrative damage of scaffolding or cytoskeleton proteins—may contribute to mitochondrial damage and/or to the disorganization of the network (20) as actin is involved in mitochondria function and dynamics (48) and α-tubulin nitration is linked to altered cell morphology, microtubule disorganization and redistribution of the motor protein dynein (49). This scenario seems to reconcile the defects at the level of cytoskeletal organization (1), mitochondrial network (20) and bioenergetics (20, 21, 24) described in cells from premutation carriers. Furthermore, considering that FMRP regulates the organization and dynamics of actin filaments (50,51), a key process in the morphogenesis of dendritic spines (50), and that actin seems to be involved in mitochondria function and dynamics (48,52–57), it could be hypothesized that altered cytoskeletal organization—as a result of nitrative damage of scaffolding proteins—could contribute to the damage to mitochondria and their network (25) as it has been reported for neurons with cytoskeletal abnormalities (58). As cytoskeletal proteins in neurons are essential for many fundamental cellular and developmental processes (that is, migration, polarity, differentiation) (59), it is possible that an altered cytoskeletal organization would also affect neurons maintenance and remodeling, contributing to the neurodegenerative clinical phenotypes associated with FXTAS.

Significant recovery of mitochondrial mass and/or function was obtained by overexpressing MIA40, or with antioxidant treatments with superoxide or hydroxyl radicals' scavengers and a glutathione peroxidase analog. While further experiments are granted to ascertain why MIA40 was underexpressed in carriers, based on the increased ROS production, it is possible that the lower MIA40 content reflects a failed oxidative protein folding leading to the formation of aggregates that are rapidly cleared by proteolysis. It is relevant to point out that MDRS defects may also elicit deficits not confined to Complex I or IV, for the MDRS-dependent small chaperone translocon of the inner membrane (TIM) is required for the import of matrix and inner membrane subunits providing an explanation for deficits in Complexes other than I and IV and MnSOD observed in fibroblasts from older carriers (21). Treatment of premutation fibroblasts with antioxidants quenching superoxide anion (MnTBAP), hydroxyl radical (dimethylsulfoxide, DMSO and Trolox), hydrogen peroxide (glutathione peroxidase peroxidase mimetic Ebselen) or ascorbic acid (to improve reducing conditions in polar phases) restored citrate synthase activity to or above control values. These results were consistent with the increased ROS detected by EPR, the lower levels of MnSOD in carriers (24) and the reported peroxyl and alkoxyl radicals-mediated oxidative modification/inactivation of citrate synthase (60). The effects of others, namely *N*-acetyl-cysteine, quercetin and epigallocatechin-3-gallate seemed to be outcome- and/or carrier-specifics (for example, age, sex, presence of FXTAS).

The effect of ethanol, tested as a putative hydroxyl radical scavenger, on the recovery of mitochondrial mass/function in cells from premutation carriers was deleterious in all cell lines from carriers. This can be explained considering that during the catabolism of ethanol to acetaldehyde and acetate, altered [NADH]/[NAD^+] ratios in cytosol and mitochondria prevent pyruvate entry into the Krebs' cycle resulting in lactate increases (Figure 4). In the presence of mitochondrial dysfunction, ethanol catabolism compounds those deficits, challenging the recovery of mitochondrial outcomes. In this context, it would be of extreme interest to evaluate whether carriers that do develop FXTAS or those that have a higher morbidity are regular consumers of alcoholic beverages. Consistent with this view, a higher rate of alcohol abuse has been reported for carriers accompanied by earlier FXTAS onset or more rapid progression (1).

CONCLUSION

Our study discusses the potential beneficial use of antioxidants and/or genetic manipulation at improving mitochondrial function, especially in relatively young subjects carrying the premutation, with low CGG repeats and before significant clinical manifestations are evident. Our findings open the door for the use of a tailored (also known by the term "precision medicine") and early intervention with antioxidants which could be crucial at preventing mitochondrial damage or rescuing mitochondrial function, especially when used in young carriers with relatively moderate CGG expansions and before the clinical involvement is evident. If replicated in larger prospective studies, the design of early interventions with antioxidant therapies or genetic manipulation to avoid cumulative damage may allow delaying the onset of FXTAS and/or decreasing its morbidity.

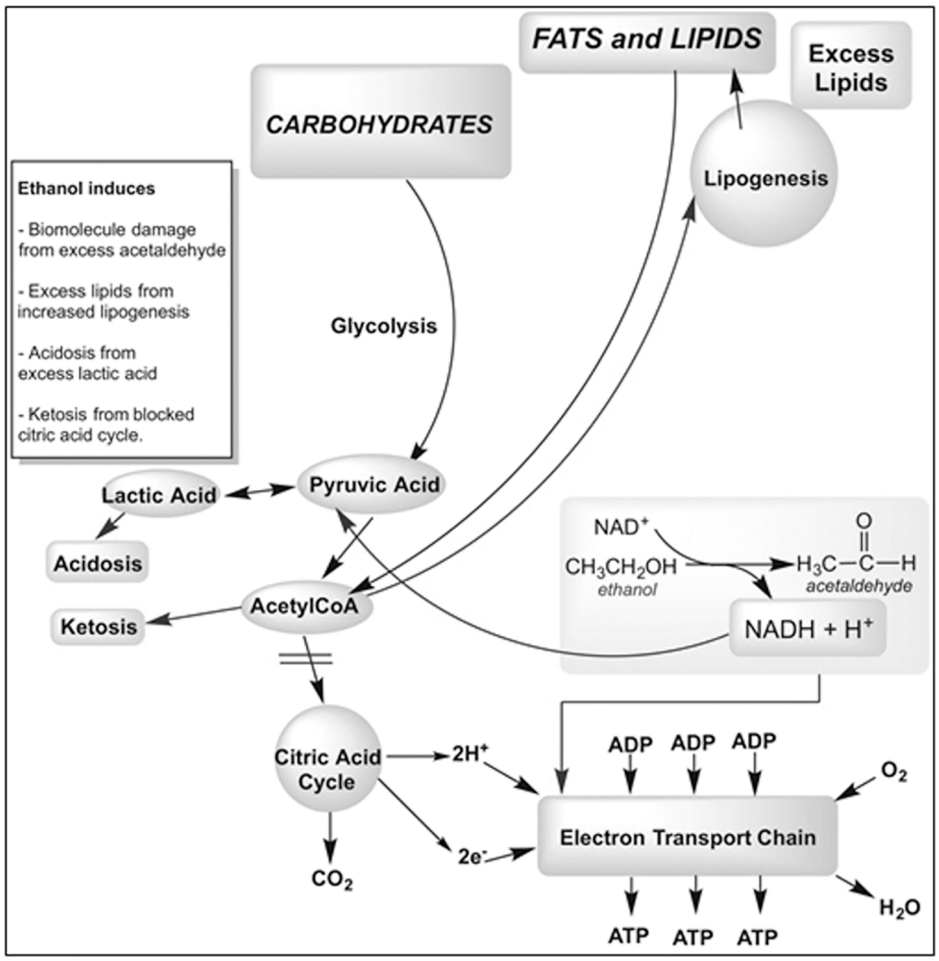

Figure 4. Ethanol metabolism in cells from premutation carriers. Ethanol is normally metabolized to acetate by generating NADH. Excess of (NADH)/(NAD^+) promotes lactate formation, inhibits Kreb's cycle, favors ketogenesis and lipogenesis from excess of acetylCoA that did not enter the Kreb's cycle. These effects are all compounded in a background exhibiting a mitochondrial dysfunction.

ACKNOWLEDGMENTS

We wish to thank all families that provided these samples making this study possible. We also thank Dr. Paul Hagerman and Ms. Glenda M Espinal (Department of Biochemistry and Molecular Medicine, University of California, Davis, School of Medicine) for providing the majority of the fibroblasts used in this study, and Ms. Stephanie Hang and Mr. Jacob Eisner (participant of the Young Scholar Program from the University of California Davis) for providing valuable technical assistance with some of the experiments. Support for this study was provided by the National Institutes of Health (S10RR023586, ES12691, HD036071 and HD040661) and, partly by the Simons Foundation (#271406). Support was also obtained from the MIND Institute Intellectual and Developmental Disabilities Research Center (U54 HD079125) and the Health and Human Administration of Developmental Disabilities grant 90DD0596.

DISCLOSURE

RH has received funding from Novartis, Roche/Genentech, Alcobra and Neuren for treatment trials in fragile X syndrome, autism and Down syndrome. She has also consulted with Novartis, Roche/Genentech and Zynerba regarding treatment for fragile X syndrome.

REFERENCES

1. Hagerman PJ, Hagerman RJ. (2015) Fragile X-associated tremor/ataxia syndrome. *Ann. N. Y. Acad. Sci.* 1338:58–70.
2. Cornish K, *et al.* (2005) The emerging fragile X premutation phenotype: evidence from the domain of social cognition. *Brain Cogn.* 57:53–60.
3. Hessl D, *et al.* (2005) Abnormal elevation of FMR1 mRNA is associated with psychological symptoms in individuals with the fragile X premutation. *Am. J. Med. Genet B. Neuropsychiatr. Genet.* 139B: 115–21.
4. Grigsby J, *et al.* (2006) Impairment in the cognitive functioning of men with fragile X-associated tremor/ataxia syndrome (FXTAS). *J. Neurol. Sci.* 248:227–33.
5. Grigsby J, *et al.* (2006) Cognitive impairment in a 65-year-old male with the fragile X-associated tremor-ataxia syndrome (FXTAS). *Cogn. Behav. Neurol.* 19:165–71.
6. Sullivan AK, *et al.* (2005) Association of FMR1 repeat size with ovarian dysfunction. *Hum. Reprod.* 20:402–12.
7. Hagerman RJ, *et al.* (2001) Intention tremor, parkinsonism, and generalized brain atrophy in male carriers of fragile X. *Neurology.* 57:127–30.
8. Jacquemont S, *et al.* (2003) Fragile X premutation tremor/ataxia syndrome: molecular, clinical, and neuroimaging correlates. *Am. J. Hum. Genet.* 72:869–78.
9. Bacalman S, *et al.* (2006) Psychiatric phenotype of the fragile X-associated tremor/ataxia syndrome (FXTAS) in males: newly described fronto-subcortical dementia. *J. Clin. Psychiatry.* 67:87–94.
10. Sutcliffe JS, *et al.* (1992) DNA methylation represses FMR-1 transcription in fragile X syndrome. *Hum. Mol. Genet.* 1:397–400.
11. Pieretti M, *et al.* (1991) Absence of expression of the FMR-1 gene in fragile X syndrome. *Cell.* 66:817–22.
12. Tassone F, *et al.* (2000) Fragile X males with unmethylated, full mutation trinucleotide repeat expansions have elevated levels of FMR1 messenger RNA. *Am. J. Med. Genet.* 94:232–6.
13. Tassone F, *et al.* (2000) Elevated levels of FMR1 mRNA in carrier males: a new mechanism of involvement in the fragile-X syndrome. *Am. J. Hum. Genet.* 66:6–15.
14. Tassone F, *et al.* (2007) Elevated FMR1 mRNA in premutation carriers is due to increased transcription. *RNA.* 13:555–62.
15. Tassone F, Iwahashi C, Hagerman PJ. (2004) FMR1 RNA within the intranuclear inclusions of fragile X-associated tremor/ataxia syndrome (FXTAS). *RNA Biol.* 1:103–5.
16. Hagerman R, Hagerman P. (2013) Advances in clinical and molecular understanding of the FMR1 premutation and fragile X-associated tremor/ataxia syndrome. *Lancet Neurol.* 12:786–98.

17. Sellier C, *et al.* (2013) Sequestration of DROSHA and DGCR8 by Expanded CGG RNA Repeats Alters MicroRNA Processing in Fragile X-Associated Tremor/Ataxia Syndrome. *Cell Rep.* 3:869–80.
18. Sellier C, *et al.* (2010) Sam68 sequestration and partial loss of function are associated with splicing alterations in FXTAS patients. *EMBO J.* 29:1248–61.
19. Berman RF, *et al.* (2014) Mouse models of the fragile X premutation and fragile X-associated tremor/ataxia syndrome. *J. Neurodev. Disord.* 6:25.
20. Napoli E, Song G, Wong S, Hagerman R, Giulivi C. (2016) Altered Bioenergetics in Primary Dermal Fibroblasts from Adult Carriers of the FMR1 Premutation Before the Onset of the Neurodegenerative Disease Fragile X-Associated Tremor/Ataxia Syndrome. *Cerebellum.* In press.
21. Napoli E, *et al.* (2011) Altered zinc transport disrupts mitochondrial protein processing/import in fragile X-associated tremor/ataxia syndrome. *Hum. Mol. Genet.* 20:3079–92.
22. Ariza J, *et al.* (2015) Dysregulated iron metabolism in the choroid plexus in fragile X-associated tremor/ataxia syndrome. *Brain Res.* 1598:88–96.
23. Kaplan ES, *et al.* (2012) Early mitochondrial abnormalities in hippocampal neurons cultured from Fmr1 pre-mutation mouse model. *J. Neurochem.* 123:613–21.
24. Ross-Inta C, *et al.* (2010) Evidence of mitochondrial dysfunction in fragile X-associated tremor/ataxia syndrome. *Biochem. J.* 429:545–52.
25. Napoli E, *et al.* (2016) Premutation in the Fragile X Mental Retardation 1 (FMR1) Gene Affects Maternal Zn-milk and Perinatal Brain Bioenergetics and Scaffolding. *Front. Neurosci.* 10:159.
26. Greco CM, *et al.* (2006) Neuropathology of fragile X-associated tremor/ataxia syndrome (FXTAS). *Brain.* 129:243–55.
27. Napoli E, *et al.* (2016) Premutation in the Fragile X Mental Retardation 1 (FMR1) Gene Affects Maternal Zn-milk and Perinatal Brain Bioenergetics and Scaffolding. *Front. Neurosci.* 10.
28. Wong S, Giulivi C. (2016) Autism, mitochondria and polybrominated diphenyl ether exposure. *CNS Neurol. Disord. Drug Targets*.
29. Johri A, Beal MF. (2012) Mitochondrial dysfunction in neurodegenerative diseases. *J. Pharmacol. Exp. Ther.* 342:619–30.
30. Tassone F, Pan R, Amiri K, Taylor AK, Hagerman PJ. (2008) A rapid polymerase chain reaction-based screening method for identification of all expanded alleles of the fragile X (FMR1) gene in newborn and high-risk populations. *J. Mol. Diagn.* 10:43–49.
31. Suthanthiran M, *et al.* (1984) Hydroxyl radical scavengers inhibit human natural killer cell activity. *Nature.* 307:276–78.
32. Albano E, Tomasi A, Goria-Gatti L, Dianzani MU. (1988) Spin trapping of free radical species produced during the microsomal metabolism of ethanol. *Chem. Biol. Interact.* 65:223–34.
33. Oldfield FF, Cowan DL, Sun AY. (1991) The involvement of ethanol in the free radical reaction of 6-hydroxydopamine. *Neurochem. Res.* 16:83–7.
34. Ingelman-Sundberg M, Johansson I. (1984) Mechanisms of hydroxyl radical formation and ethanol oxidation by ethanol-inducible and other forms of rabbit liver microsomal cytochromes P-450. *J. Biol. Chem.* 259:6447–58.
35. Miller GG, Raleigh JA. (1983) Action of some hydroxyl radical scavengers on radiation-induced haemolysis. *Int. J. Radiat. Biol. Relat. Stud. Phys. Chem. Med.* 43:411–19.
36. Phillis JW, Estevez AY, O'Regan MH. (1998) Protective effects of the free radical scavengers, dimethyl sulfoxide and ethanol, in cerebral ischemia in gerbils. *Neurosci. Lett.* 244:109–11.
37. Roots R, Okada S. (1972) Protection of DNA molecules of cultured mammalian cells from radiation-induced single-strand scissions by various alcohols and SH compounds. *Int. J. Radiat. Biol. Relat. Stud. Phys. Chem. Med.* 21:329–42.
38. Napoli E, *et al.* (2013) Defective mitochondrial disulfide relay system, altered mitochondrial morphology and function in Huntington's disease. *Hum. Mol. Genet.* 22:989–1004.
39. Giulivi C, *et al.* (2010) Mitochondrial dysfunction in autism. *JAMA.* 304:2389–96.
40. Napoli E, *et al.* (2015) Mitochondrial Citrate Transporter-dependent Metabolic Signature in the 22q11.2 Deletion Syndrome. *J. Biol. Chem.* 290:23240–253.
41. Napoli E, Hung C, Wong S, Giulivi C. (2013) Toxicity of the flame-retardant BDE-49 on brain mitochondria and neuronal progenitor striatal cells enhanced by a PTEN-deficient background. *Toxicol. Sci.* 132:196–210.
42. Kuznetsov AV, Margreiter R, Amberger A, Saks V, Grimm M. (2011) Changes in mitochondrial redox state, membrane potential and calcium precede mitochondrial dysfunction in doxorubicin-induced cell death. *Biochim. Biophys. Acta.* 1813:1144–52.
43. Todd PK, *et al.* (2013) CGG repeat-associated translation mediates neurodegeneration in fragile X tremor ataxia syndrome. *Neuron.* 78:440–55.
44. Napierala M, Michalowski D, de Mezer M, Krzyzosiak WJ. (2005) Facile FMR1 mRNA structure regulation by interruptions in CGG repeats. *Nucleic Acids Res.* 33:451–63.
45. Weisman-Shomer P, Cohen E, Fry M. (2000) Interruption of the fragile X syndrome expanded sequence d(CGG)(n) by interspersed d(AGG) trinucleotides diminishes the formation and stability of d(CGG)(n) tetrahelical structures. *Nucleic Acids Res.* 28:1535–41.
46. Sellier C, *et al.* (2014) The multiple molecular facets of fragile X-associated tremor/ataxia syndrome. *J. Neurodev. Disord.* 6:23.
47. Conca Dioguardi C, Uslu, B., Haynes, M., Kurus, M., Gul, M., Miao, D-Q., De Santis, L., Ferrari, M., Bellone, S., Santin, A., Giulivi, C., Hoffman, G., Usdin, K. and Johnson, J. (2016) Granulosa cell and oocyte mitochondrial abnormalities in a mouse model of fragile X primary ovary insufficiency. *Mol. Hum. Reprod.* 22:384–96.
48. Hatch AL, Gurel PS, Higgs HN. (2014) Novel roles for actin in mitochondrial fission. *J. Cell. Sci.* 127:4549–60.
49. Eiserich JP, *et al.* (1999) Microtubule dysfunction by posttranslational nitrotyrosination of alpha-tubulin: a nitric oxide-dependent mechanism of cellular injury. *Proc. Natl. Acad. Sci. U. S. A.* 96:6365–70.
50. Castets M, *et al.* (2005) FMRP interferes with the Rac1 pathway and controls actin cytoskeleton dynamics in murine fibroblasts. *Hum. Mol. Genet.* 14:835–44.
51. Nolze A, *et al.* (2013) FMRP regulates actin filament organization via the armadillo protein p0071. *RNA.* 19:1483–96.
52. Xu X, Forbes JG, Colombini M. (2001) Actin modulates the gating of Neurospora crassa VDAC. *J. Membr. Biol.* 180:73–81.
53. Dugina V, Zwaenepoel I, Gabbiani G, Clement S, Chaponnier C. (2009) Beta and gamma-cytoplasmic actins display distinct distribution and functional diversity. *J. Cell. Sci.* 122:2980–88.
54. Korobova F, Ramabhadran V, Higgs HN. (2013) An actin-dependent step in mitochondrial fission mediated by the ER-associated formin INF2. *Science.* 339:464–67.
55. Boldogh IR, Pon LA. (2006) Interactions of mitochondria with the actin cytoskeleton. *Biochim. Biophys. Acta.* 1763:450–62.
56. Higuchi R, *et al.* (2013) Actin dynamics affect mitochondrial quality control and aging in budding yeast. *Curr. Biol.* 23:2417–22.
57. Li J, *et al.* (2004) Beta-actin is required for mitochondria clustering and ROS generation in TNF-induced, caspase-independent cell death. *J. Cell. Sci.* 117:4673–80.
58. Anesti V, Scorrano L. (2006) The relationship between mitochondrial shape and function and the cytoskeleton. *Biochim. Biophys. Acta.* 1757:692–699.
59. Kapitein LC, Hoogenraad CC. (2015) Building the *Neuron*al Microtubule Cytoskeleton. *Neuron.* 87:492–506.
60. Chepelev NL, Bennitz JD, Wright JS, Smith JC, Willmore WG. (2009) Oxidative modification of citrate synthase by peroxyl radicals and protection with novel antioxidants. *J. Enzyme. Inhib. Med. Chem.* 24:1319–31.

Cite this article as: Song G, *et al.* (2016) Altered redox mitochondrial biology in the neurodegenerative disorder fragile X-Tremor/Ataxia syndrome: Use of antioxidants in precision medicine. *Mol. Med.* 22:548–59.